

Supplementary Information

for

**Chemical Activation of Atom-Precise Pd₃ Nanoclusters on γ -Al₂O₃
Supports for Transfer Hydrogenation Reactions**

Siddhant Singh^a, Dami Wi^a, Kholoud E. Salem^b, Drew Higgins^b, and Robert W. J. Scott*^a

^a Department of Chemistry, University of Saskatchewan, 110 Science Place, Saskatoon, Saskatchewan S7N 5C9, Canada. E-mail: robert.scott@usask.ca

^b Department of Chemical Engineering, McMaster University, 1280 Main St W, Hamilton, Ontario L8S 4L7, Canada

S1. Experimental

Triphenylphosphine (PPh₃, ≥99%), palladium(II) chloride (99.9% on a metal basis), sodium borohydride (NaBH₄, 98%), lithium borohydride solution (LiBH₄, 2.0 M in THF), lithium aluminum hydride solution (LiAlH₄, 2.0 M in THF), aluminum oxide (γ-Al₂O₃ pore size: 58 Å, mesh size: 150), hydrochloric acid (HCl, > 99%), nitric acid (HNO₃ > 99%) and *trans*-cinnamaldehyde (CAL, 97%) were procured from Sigma-Aldrich. All the organic solvents, i.e., tetrahydrofuran (THF, ACS grade), hexanes (ACS grade), diethyl ether (HPLC grade), toluene (ACS grade), ethanol (EtOH, ACS grade), dichloromethane (DCM, ACS grade), and methanol (MeOH, ACS grade) were purchased from Fisher Scientific and used without any purification. All the bases and hydrogen donors i.e., formic acid (HCOOH, LC/MS grade), anhydrous sodium carbonate, (Na₂CO₃, ACS grade), sodium hydroxide (NaOH, 98%), potassium hydroxide (KOH, ACS grade), sodium formate (HCOONa, 98%) and ammonium formate (HCOONH₄, 98%) were purchased from ThermoFisher Scientific. Milli-Q (Millipore, Bedford, MA) water with a resistivity of 18.2 MΩ cm was used in all the experiments.

S1.1. Synthesis of Pd₃ NCs. The synthesis of [Pd₃(μ-Cl)(μ-PPh₂)₂(PPh₃)₃]Cl NCs (Pd₃ NCs) was carried out by following a previously reported procedure.¹ In the first step, 0.6 mL of a 0.8 mM solution of PdCl₂ in concentrated HCl was added to 10 mL of THF. After stirring the above solution for 5 min, 1.2 mmol of triphenylphosphine was added quickly to the solution. After that, the colour of the solution turned from dark brown to light yellow indicating the formation of the Pd-phosphine complex. The solution was further stirred for 5 mins at room temperature followed by an addition of 5.0 mL of 0.4 mM NaBH₄ in EtOH. The addition of NaBH₄ turned the colour of the solution to black. The solution was further stirred at room temperature for 1 h followed by centrifugation to remove the excess phosphines as solids. The remaining solution was evaporated in the rotavap and 10 mL of DCM was added to the obtained solid. Thereafter, the DCM solution was washed with 3 portions of 20 mL of water. After evaporating the DCM from the mixture, the remaining solid was dissolved in 3 mL of the EtOH, and the Pd₃ NCs were precipitated as an orange powder by adding hexanes dropwise to the solution. (isolated yield: 53.6%)

S1.2. Synthesis of Pd₃/Al₂O₃. For immobilizing the Pd NCs on the γ -Al₂O₃ surface, the Pd NCs (10.0 mg) were first dissolved in 5.0 mL of ethanol. Under vigorous stirring, 100 mg of γ -Al₂O₃ support was added to the mixture, and the solution was stirred for 4 h at room temperature followed by gravity filtration to obtain Pd₃/Al₂O₃.

S1.3. Chemical Activation of Pd₃/Al₂O₃. To chemically activate the Pd₃/Al₂O₃, 500 mg of supported catalyst was dispersed in the respective solvent (**Table S1**) under sonication for 5 min. Thereafter, the mixture was transferred into a two-neck flask. The ends of the flask were sealed using rubber septa. The solution of the respective reducing agent (freshly prepared NaBH₄ in water or LiBH₄/LiAlH₄ in THF) was added to the flask using a syringe under a gentle flow of N₂ to avoid H₂ buildup in the flask. After 1 h, the reaction mixture was filtered using Buchner filtration and washed with 3×10mL portions of ethanol, diethyl ether, and water.

Table S1. Different combinations of solvents, reducing agents and their concentrations used for the activation of Pd₃ NCs.

Catalyst	Reducing Agent	Solvent Used	Pd: Reducing Agent moles (approx.)	Amount of Reducing Agent
Pd ₃ /Al ₂ O ₃ -NaBH ₄ (A)	NaBH ₄	DI water	1:300	3.0 mL of 2.2 M solution in water*
Pd ₃ /Al ₂ O ₃ -NaBH ₄ (B)	NaBH ₄	DI water	1:600	3.0 mL of 4.4 M solution in water*
Pd ₃ /Al ₂ O ₃ -NaBH ₄ (C)	NaBH ₄	DI water	1:1200	3.0 mL of 8.8 M solution in water*
Pd ₃ /Al ₂ O ₃ -LiBH ₄ (A)	LiBH ₄	Diethyl ether	1:10	0.10 mL of 2.0 M solution in THF
Pd ₃ /Al ₂ O ₃ -LiBH ₄ (B)	LiBH ₄	Diethyl ether	1:50	0.50 mL of 2.0 M solution in THF
Pd ₃ /Al ₂ O ₃ -LiBH ₄ (C)	LiBH ₄	Diethyl ether	1:100	1.00 mL of 2.0 M solution in THF
Pd ₃ /Al ₂ O ₃ -LiAlH ₄ (A)	LiAlH ₄	Diethyl ether	1:10	0.10 mL of 2.0 M solution in THF
Pd ₃ /Al ₂ O ₃ -LiAlH ₄ (B)	LiAlH ₄	Diethyl ether	1:50	0.50 mL of 2.0 M solution in THF
Pd ₃ /Al ₂ O ₃ -LiAlH ₄ (C)	LiAlH ₄	Diethyl ether	1:100	1.00 mL of 2.0 M solution in THF
*Freshly prepared solution				

S.1.3 Catalyst Evaluation for the transfer-hydrogenation of cinnamaldehyde. For transfer-hydrogenation reactions, 1.0 mmol of trans-cinnamaldehyde was dissolved in the desired solution inside a 25 mL round-bottom flask. Thereafter, 25.0 mg of the Pd₃/Al₂O₃ catalyst was added to the mixture followed by the desired base/additives (**Tables 2 and 3**). The round-bottom flask was then heated at 70 °C in a cold-water condenser unit for 3 h. After the completion of the reaction, 2.0 mL of the reaction mixture was then filtered using a 0.2 μM PTFE syringe filter and the reaction products were analyzed by GC-FID.

S2. Characterization

For elemental analysis, 50 mg of the Pd₃/Al₂O₃ was digested in 10 mL of aqua regia (1 : 3 HNO₃ : HCl). PdCl₂ was used for making standard solutions. A Varian SpectrAA 55 Atomic Absorption Spectroscopy equipped with a multielement hollow cathode lamp was used to analyze the concentration of Pd in the sample. X-ray Photoelectron Spectroscopy (XPS) analysis was performed using a Kratos (Manchester, UK) AXIS Supra system equipped with a 500 mm Rowland circle monochromatic Al Kα (1486.6 eV) source and combined hemispherical analyzer and spherical mirror analyzer. XPS data analysis and fitting were performed using the CasaXPS software package.² For calibrating the XPS data, C 1s regions were collected for each sample, and adventitious carbon was fitted at 284.8 eV. Pd K edge X-ray absorption spectroscopy (XAS) analysis was performed at Hard X-ray MicroAnalysis beamline (HXMA, energy range 5–40 keV; resolution $1 \times 10^{-4} \Delta E/E$; spot size 0.8 mm × 1.5 mm (W × H)) at the Canadian Light Source. For the selection of the correct energy range, a Si (111) double crystal monochromator with an Rh-coated KB mirror was used. All the data was collected in fluorescence mode using a 13-element Ge detector. Data analysis and Extended X-ray absorption fine structure (EXAFS) fitting were carried out using the Demeter software package.³ For EXAFS fitting, the amplitude reduction factor of Pd was obtained from fitting Pd foil and fixed at 0.78 during the fitting of samples. For calculation of the conversion and selectivity percentages of catalytic reactions, GC analyses were performed using Agilent 7890A GC system equipped with a flame ionization detector (FID) and Agilent HP-INNOWax column. Calibration curves were made using commercially available reagents for both substrates and products. The morphological characterization and elemental mapping of the activated Pd NCs catalysts were carried out using high-resolution transmission electron microscope (HR-TEM), high-angle annular dark-field scanning transmission microscopy

(HAADF-STEM) imaging, along with energy dispersive X-ray (EDX) mapping. All TEM and HAADF-STEM-EDX characterizations were performed using Thermo Scientific Talos 200X operates at 200kV available at the Canada Center for Electron Microscopy at McMaster University. STEM-EDX elemental maps of the STEM images displaying the intensity of X-ray counts associated with Pd $K\alpha$, B $K\alpha$, Al $K\alpha$, and O $K\alpha$ peaks. The EDX mapping was acquired using a 4 SDD (Silicon Drift Detector) symmetric design, which is windowless and shutter-protected. Powder samples were prepared in ethanol to form an ink, the ink was sonicated for 10 minutes before drop-casting a 1 -2 μL drop on a 400-mesh copper grid and drying for an hour. The average particle size was determined using ImageJ software.

S3. Wavelet Transform Analysis of EXAFS data

For the samples having either several scattering pathways of different atomic species with atomic number difference less than 5 (i.e., identical amplitude function) or multiple scattering pathways present at the same region of R space, it can be challenging to assign peaks unambiguously. This is majorly due to the overlapping of the multiple scattering pathways resulting in a distorted Fourier Transform (FT) peak in the R-space EXAFS spectrum.⁴ In such cases, Wavelet Transform (WT) of EXAFS analysis can show the areas in k space responsible for the FT peak. This way one can clearly observe the number of distinct types of back scatterers.⁴ Two different values of η and σ have been used to calculate the WT in this work. $\eta = 10.5$ (frequency of the sine or cosine functions in Morlet wavelet) and $\sigma = 1.5$ (the width of the Gaussian function) provide a better resolution in R-space (scatterer distance) but poor k-space (scatterer type) resolution.^{4,5} A second set of calculations has been carried out using values of $\eta = 7.5$ and $\sigma = 0.5$, this decreases the resolution in R-space, but increases it in k-space permitting a more detailed description of the different regions of the k-space wave. In the case of Pd₃/Al₂O₃-NaBH₄ (B), two separate peak centers are present at around R= 2 - 2.5 Å indicating the presence of two scatterers (Figure S1 (f)). However, the presence of one peak center in the same region in the case of Pd₃/Al₂O₃-NaBH₄ (A) indicates the presence of one scatterer (Figure S1 (d)).

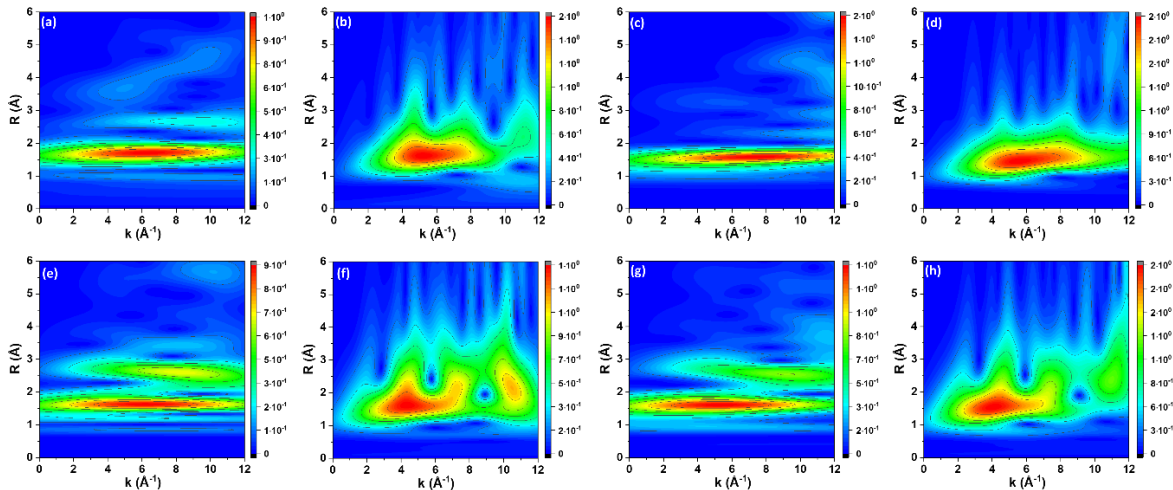


Figure S1. The Wavelet transform of the experimental EXAFS spectra at the Pd K-edge of (a) Pd₃/Al₂O₃ ($\eta = 10.5$ and $\sigma = 1.5$); (b) Pd₃/Al₂O₃ ($\eta = 7.5$ and $\sigma = 0.5$); (c) Pd₃/Al₂O₃-NaBH₄(A) ($\eta = 10.5$ and $\sigma = 1.5$); (d) Pd₃/Al₂O₃-NaBH₄(A) ($\eta = 7.5$ and $\sigma = 0.5$); (e) Pd₃/Al₂O₃-NaBH₄(B) ($\eta = 10.5$ and $\sigma = 1.5$); (f) Pd₃/Al₂O₃-NaBH₄(B) ($\eta = 7.5$ and $\sigma = 0.5$); (g) Pd₃/Al₂O₃-NaBH₄(C) ($\eta = 10.5$ and $\sigma = 1.5$) and (h) Pd₃/Al₂O₃-NaBH₄(C) ($\eta = 7.5$ and $\sigma = 0.5$).

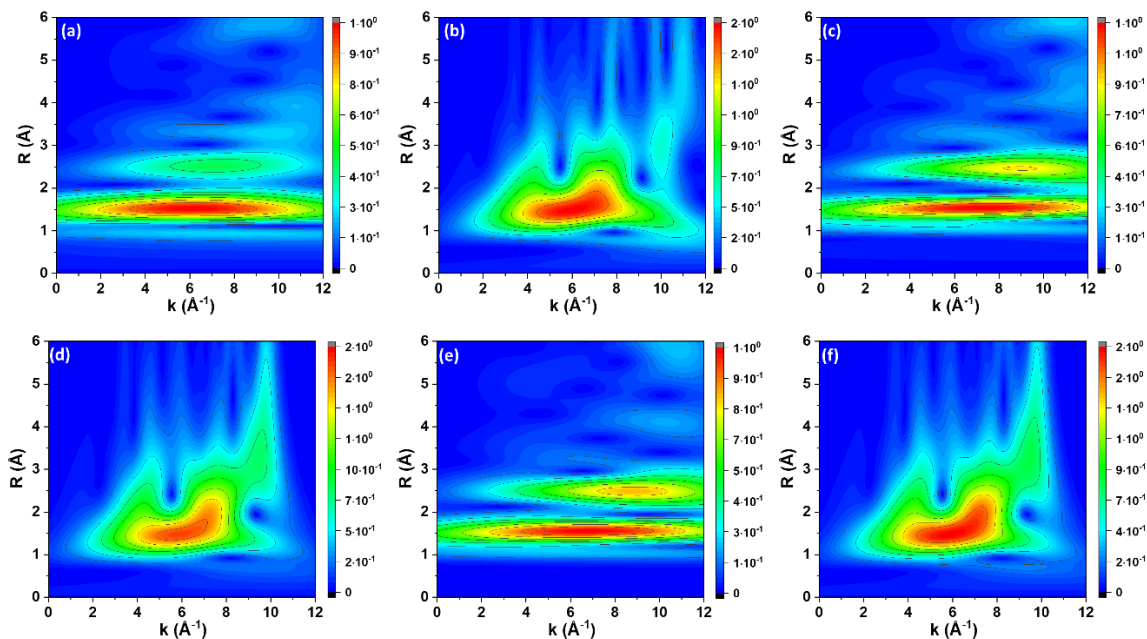


Figure S2. The Wavelet transform of the experimental EXAFS spectra at the Pd K-edge of (a) Pd₃/Al₂O₃-LiBH₄(A) ($\eta = 10.5$ and $\sigma = 1.5$); (b) Pd₃/Al₂O₃-LiBH₄(A) ($\eta = 7.5$ and $\sigma = 0.5$); (c) Pd₃/Al₂O₃-LiBH₄(B) ($\eta = 10.5$ and $\sigma = 1.5$); (d) Pd₃/Al₂O₃-LiBH₄(B) ($\eta = 7.5$ and $\sigma = 0.5$); (e) Pd₃/Al₂O₃-LiBH₄(C) ($\eta = 10.5$ and $\sigma = 1.5$) and (f) Pd₃/Al₂O₃-LiBH₄(C) ($\eta = 7.5$ and $\sigma = 0.5$).

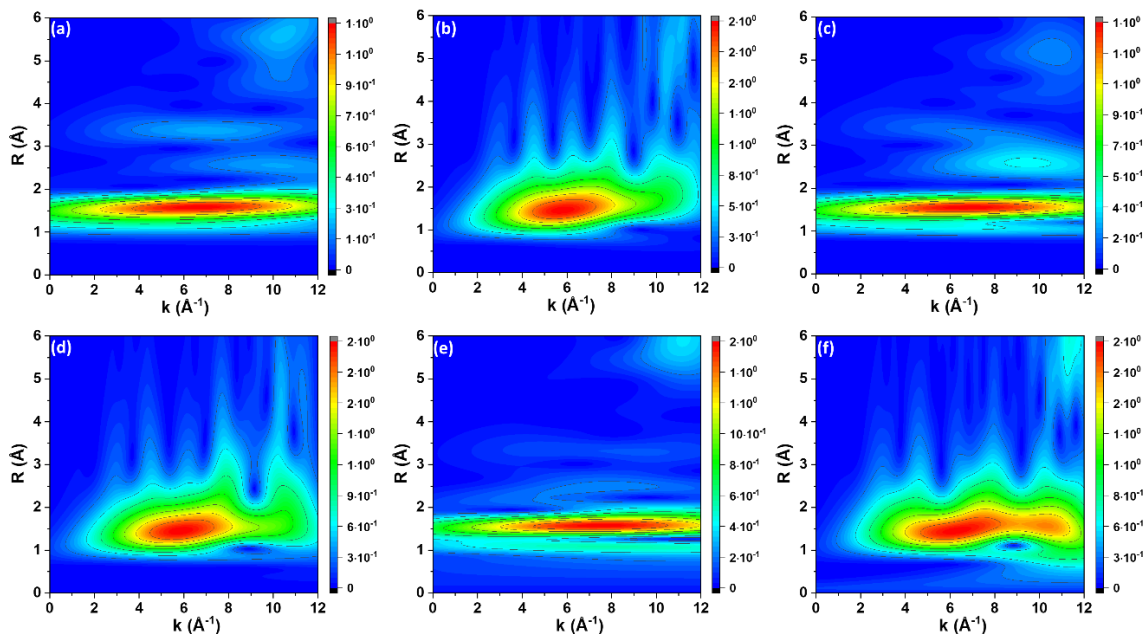


Figure S3. The Wavelet transform of the experimental EXAFS spectra at the Pd K-edge of (a) Pd₃/Al₂O₃-LiAlH₄(A) ($\eta = 10.5$ and $\sigma = 1.5$); (b) Pd₃/Al₂O₃-LiAlH₄(A) ($\eta = 7.5$ and $\sigma = 0.5$); (c) Pd₃/Al₂O₃-LiAlH₄(B) ($\eta = 10.5$ and $\sigma = 1.5$); (d) Pd₃/Al₂O₃-LiAlH₄(B) ($\eta = 7.5$ and $\sigma = 0.5$); (e) Pd₃/Al₂O₃-LiAlH₄(C) ($\eta = 10.5$ and $\sigma = 1.5$) and (f) Pd₃/Al₂O₃-LiAlH₄(C) ($\eta = 7.5$ and $\sigma = 0.5$).

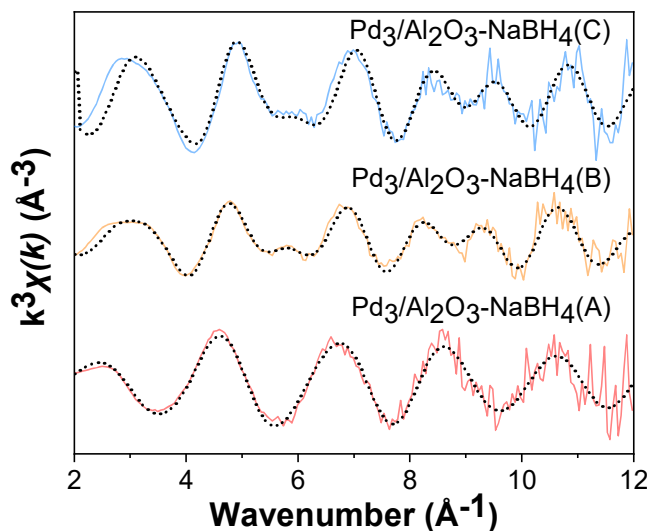


Figure S4. Fitted Pd K-edge EXAFS spectra in k-space for Pd₃/Al₂O₃ activated via treatment with different amounts of NaBH₄, where coloured solid lines represent the experimental data and black dots represent the best fit.

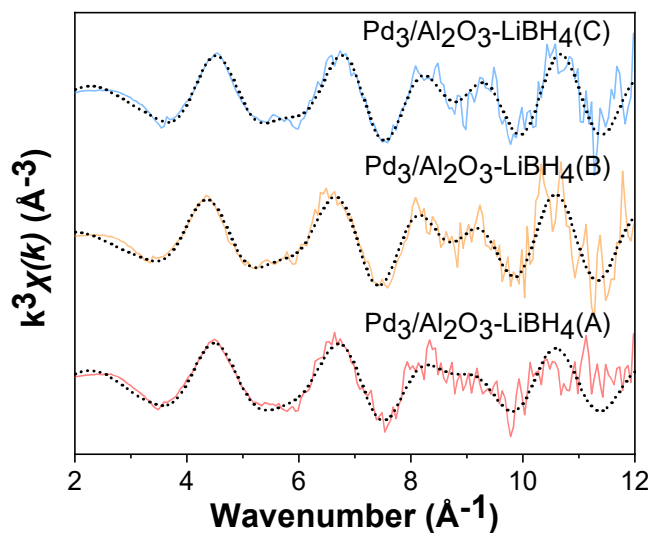


Figure S5. Fitted Pd K-edge EXAFS spectra in k-space for Pd₃/Al₂O₃ activated via treatment with different amounts of LiBH₄, where coloured solid lines represent the experimental data and black dots represent the best fit.

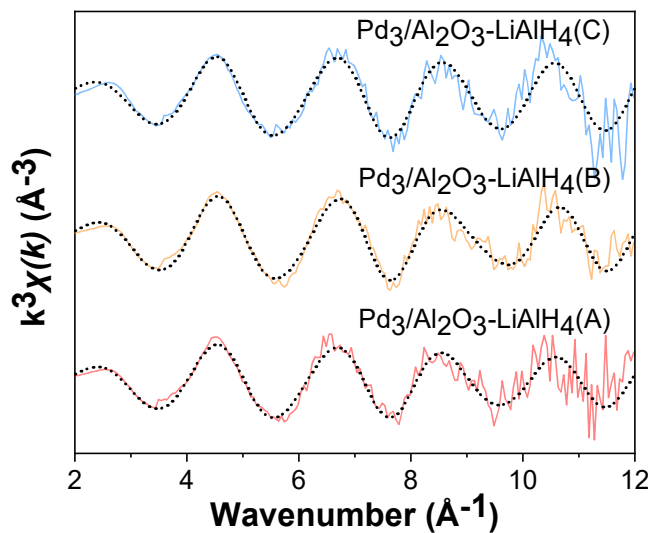


Figure S6. Fitted Pd K-edge EXAFS spectra in k-space for Pd₃/Al₂O₃ activated via treatment with different amounts of LiAlH₄, where coloured solid lines represent the experimental data and black dots represent the best fit.

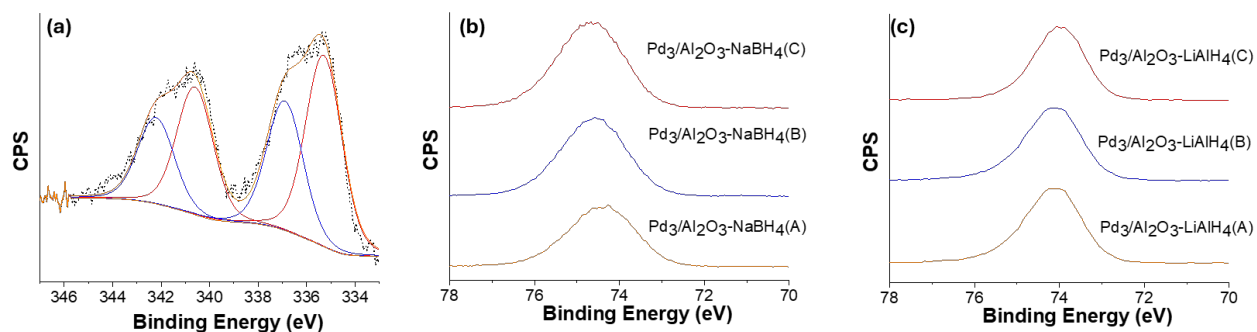


Figure S7. (a) XPS Pd 3d spectra of Pd₃/Al₂O₃-LiBH₄(B); black dots and orange solid lines represent the experiment data and fit respectively; red lines represent the 3d_{5/2} (right) and 3d_{3/2} (left) regions for Pd(0); blue lines represent the 3d_{5/2} (right) and 3d_{3/2} (left) regions for Pd(II). XPS Al 2p spectra of Pd₃/Al₂O₃ catalysts treated with (b) NaBH₄ and (c) LiAlH₄.

S4. ³¹P MAS NMR Analysis of Activated Samples-

The MAS NMR of the PPh₃ ligand (Figure S8) shows a sharp singlet at -8.97 ppm, which is in good agreement with the literature value (~9.3 ppm).⁶ The two minor peaks shown by asterisks are the spinning sidebands, arising from the chemical shift anisotropy of P nuclei.⁶ In the case of Pd₃/Al₂O₃, a peak possible due to the merging of two separate peaks can be seen around 26.4 ppm (Figure S8). The peak positions for the Pd₃ NCs adsorbed on γ -Al₂O₃ are in good agreement with the reported values for phosphine-ligated Pd complexes.⁷ Upon activation (Figure S8), the main peak for the ³¹P nuclei undergo heavy deshielding (5.6-11.7 ppm in magnitude) in comparison to non-activated Pd₃/Al₂O₃ NCs. The spinning side bands of some of the peaks still can be seen (represented by asterisks) shifted to the magnitude of ~49.5 ppm from the main peak. In the case of Pd₃/Al₂O₃-NaBH₄(B), Pd₃/Al₂O₃-NaBH₄(C), Pd₃/Al₂O₃-LiBH₄(B), and Pd₃/Al₂O₃-LiAlH₄(B), a broad peak around -5 ppm is present, which is consistent with the adsorption of PPh₃ on the surface of γ -Al₂O₃.⁶ The sharp peak present at 32-38 ppm may be due to oxidized PPh₃ and PPh₂⁻ ligands left on the alumina surface after activation.⁸

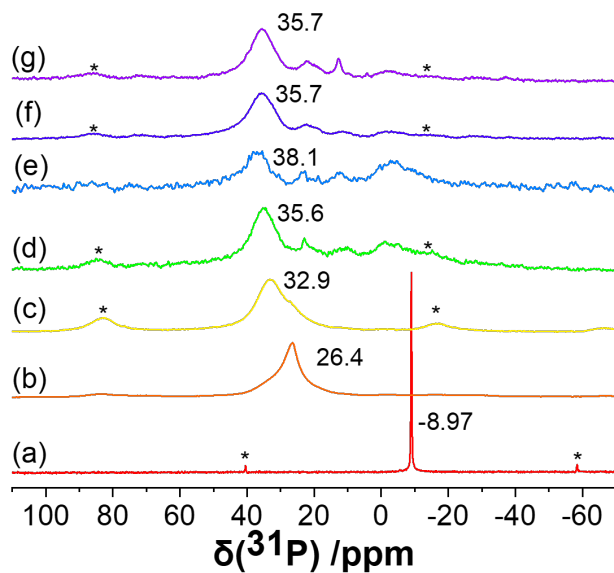


Figure S8. ^{31}P MAS NMR of (a) PPh_3 , (b) $\text{Pd}_3/\text{Al}_2\text{O}_3$, (c) $\text{Pd}_3/\text{Al}_2\text{O}_3\text{-NaBH}_4(\text{A})$, (d) $\text{Pd}_3/\text{Al}_2\text{O}_3\text{-NaBH}_4(\text{B})$, (e) $\text{Pd}_3/\text{Al}_2\text{O}_3\text{-NaBH}_4(\text{C})$, (f) $\text{Pd}_3/\text{Al}_2\text{O}_3\text{-LiBH}_4(\text{B})$ and (g) $\text{Pd}_3/\text{Al}_2\text{O}_3\text{-LiAlH}_4(\text{B})$ (asterisks represent the spinning sidebands).

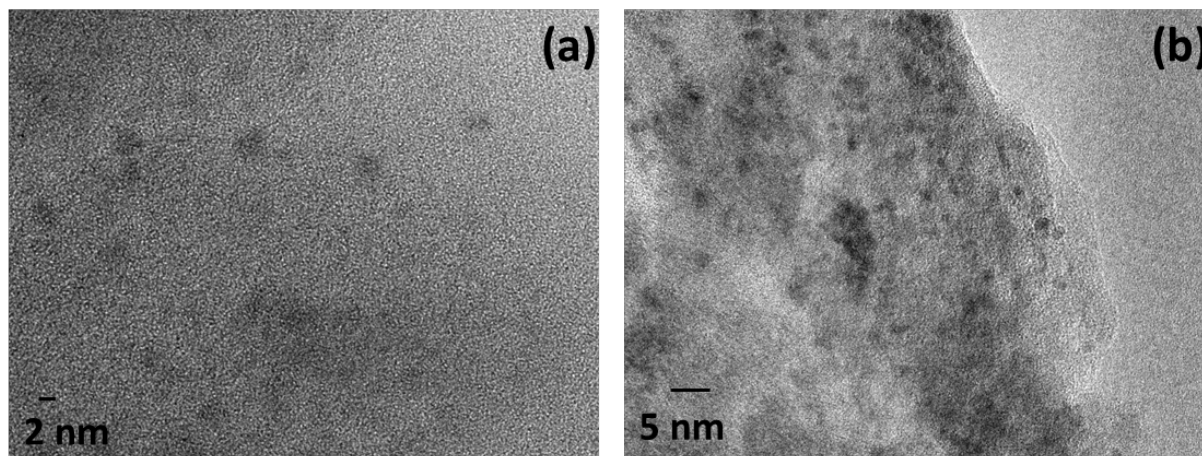


Figure S9 HR-TEM images of (a) $\text{Pd}_3/\text{Al}_2\text{O}_3\text{-NaBH}_4(\text{B})$ (Avg. Pd size: 3.2 ± 0.8 nm) and (b) $\text{Pd}_3/\text{Al}_2\text{O}_3\text{-LiBH}_4(\text{B})$ (Avg. Pd size: 2.5 ± 0.5 nm).

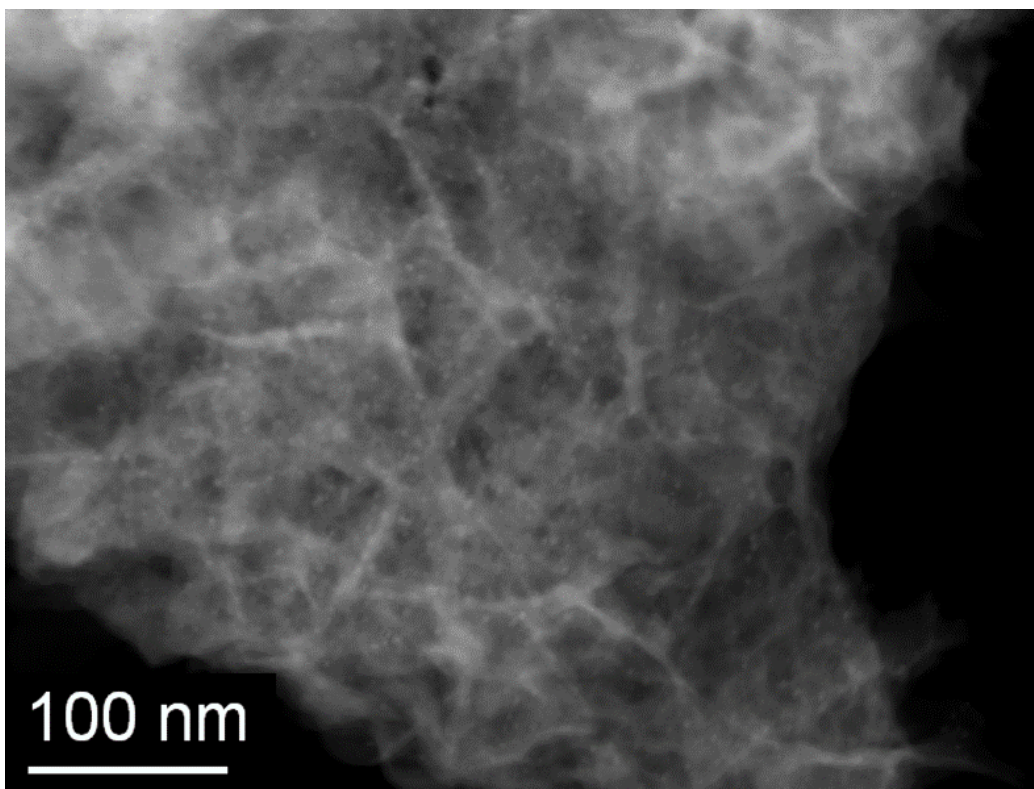


Figure S10. HAADF-STEM image of Pd₃/Al₂O₃-LiAlH₄(B).

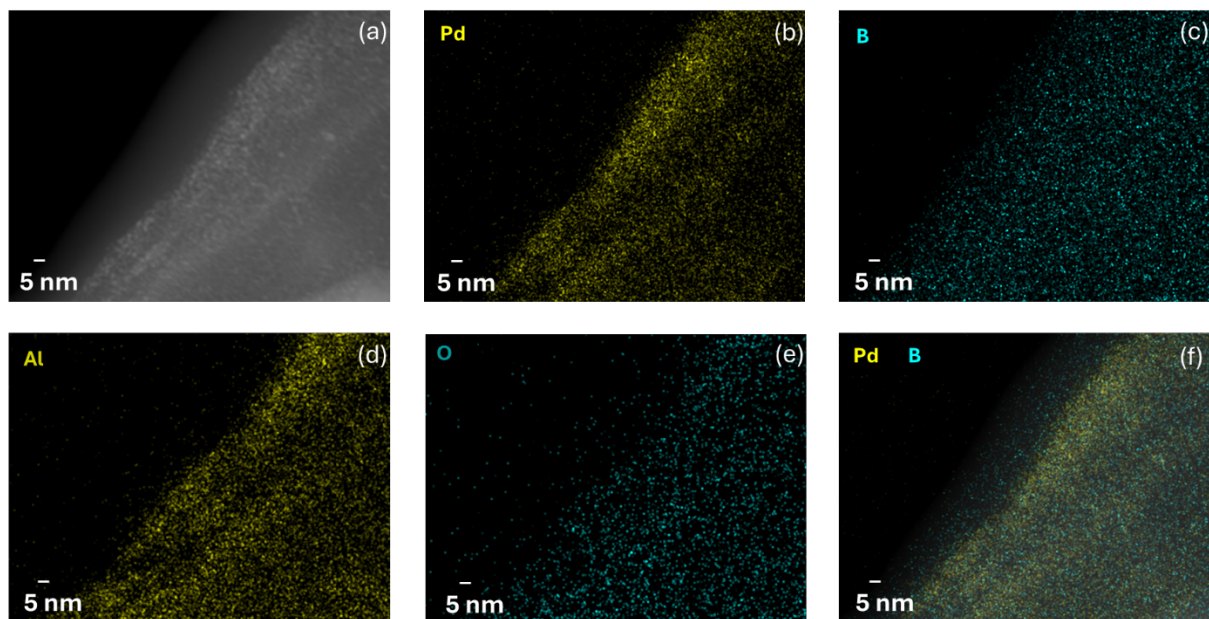


Figure S11. (a) HAADF-STEM images of the Pd₃/Al₂O₃-NaBH₄(A). (b-e) STEM-EDX mappings showing the distribution of Pd, B, Al and O in the sample. (f) Overlay of STEM-EDX maps of Pd and B.

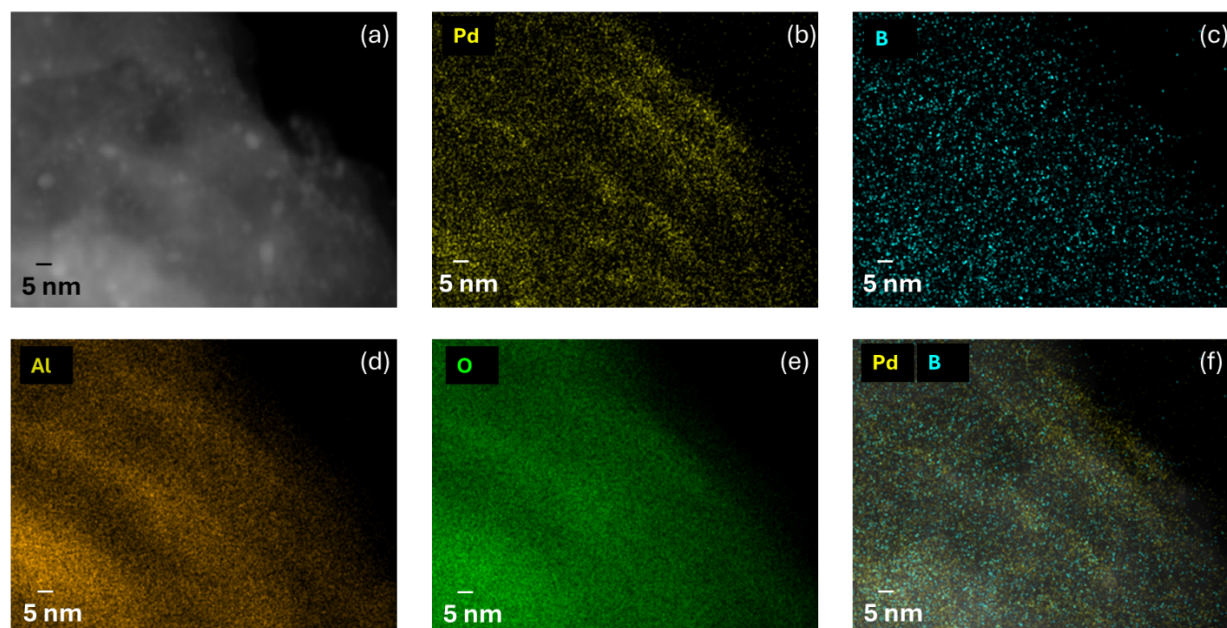


Figure S12. (a) HAADF-STEM images of the Pd₃/Al₂O₃-NaBH₄(B). (b-e) STEM-EDX mappings showing the distribution of Pd, B, Al and O in the sample. (f) Overlay of STEM-EDX maps of Pd and B.

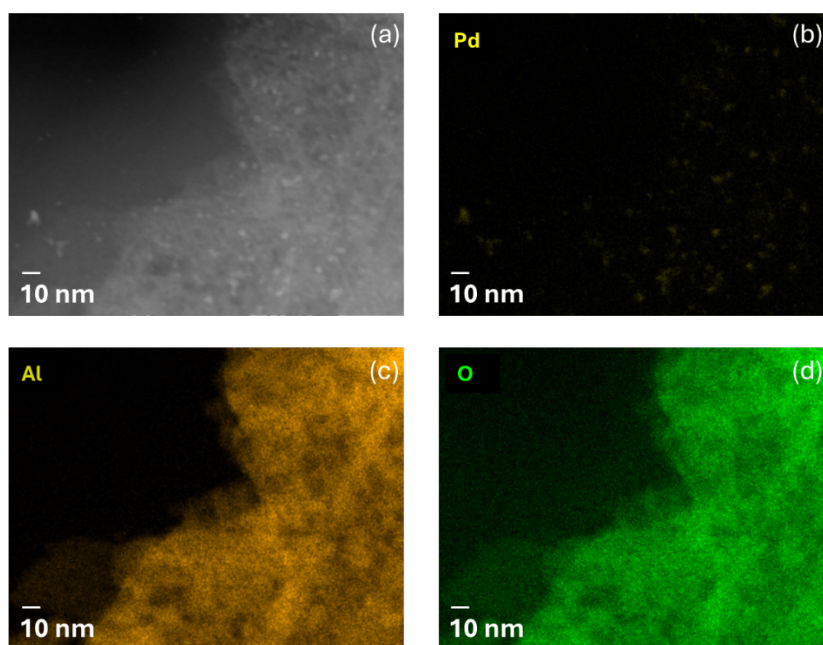


Figure S13. (a) HAADF-STEM images of the Pd₃/Al₂O₃-LiBH₄(B). (b-d) STEM-EDX mappings showing the distribution of Pd, Al and O in the sample.

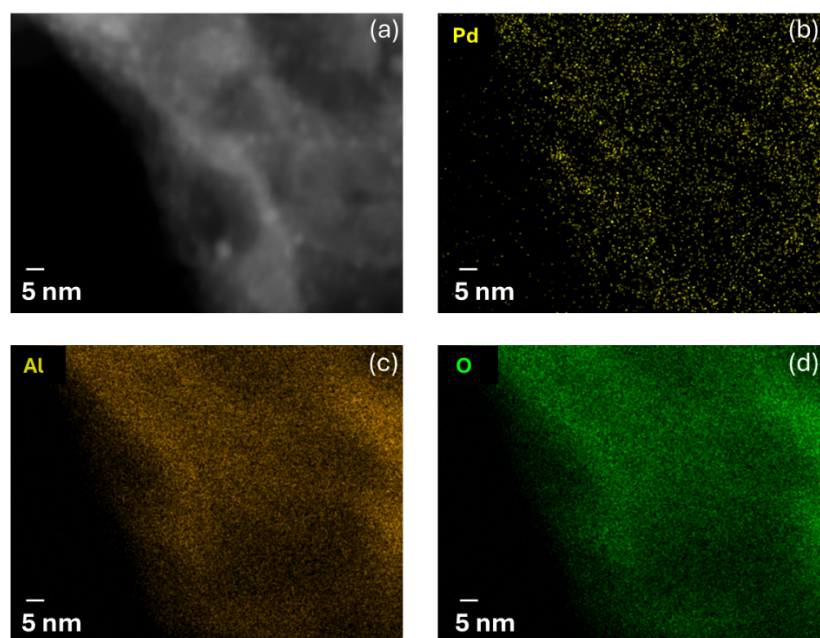
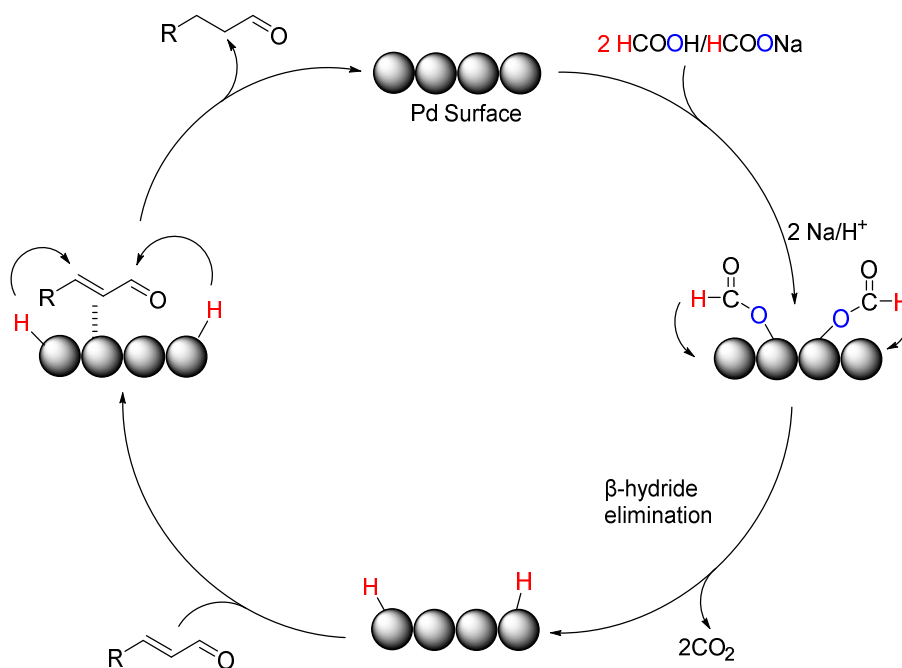


Figure S14. (a) HAADF-STEM images of the Pd₃/Al₂O₃-LiAlH₄(B). (b-d) STEM-EDX mappings showing the distribution of Pd, Al and O in the sample.

Table S2. Results of quantitative analysis of EDX spectra.

Sample	Atomic Fraction of Pd (%)	Atomic Fraction of Al (%)	Atomic Fraction of O (%)	Atomic Fraction of B (%)
Pd ₃ /Al ₂ O ₃ -NaBH ₄ (B)	0.8 ± 0.2	16 ± 4	82 ± 4	0.23 ± 0.04
Pd ₃ /Al ₂ O ₃ -LiAlH ₄ (B)	0.35 ± 0.05	33.4 ± 4.4	65 ± 4	-



Scheme S1. A plausible mechanism of the transfer-hydrogenation of CAL to HCAL on the surface of Pd catalysts using formic acid/sodium formate as the H-source. Adapted from references 9 and 10.

References

1. S. Singh, K. O. Sulaiman, Mahwar and Robert W. J. Scott, *Catal. Sci. Technol.*, 2024, **14**, 322.
2. N. Fairley, V. Fernandez, M. Richard-Plouet, C. Guillot-Deudon, J. Walton, E. Smith, D. Flahaut, M. Greiner, M. Biesinger, S. Tougaard and D. Morgan, *Appl. Surf. Sci. Adv.*, 2021, **5**, 100112.
3. B. Ravel and M. A. Newville, *J. Synchrotron Radiat.*, 2005, **12**, 537.
4. T.J. Penfold, I. Tavernelli, C.J. Milne, M. Reinhard, A. E. Nahhas, R. Abela, U. Rothlisberger and M. Chergui, *J. Chem. Phys.*, 2013, **138**, 014104.
5. H. Funke, A. Scheinost and M. Chukalina, *Phys. Rev. B*, 2005, **71**, 094110.
6. B. Hu and I.G. Gay, *Langmuir*, 1999, **15**, 477.
7. L. Bemi, H. C. Clark, J. A. Davies, C. A. Fyfe and R. E. Wasylshen, *J. Am. Chem. Soc.*, 1982, **104**, 438.
8. P. J. Hubbard, J. W. Benzie, V. I. Bakmutov and J. Blüme, *J. Chem. Phys.*, 2020, **152**, 054718.
9. R. Nie, Y. Tao, Y. Nie, T. Lu, J. Wang, Y. Zhang, X. Lu and C. C. Xu, *ACS Catal.*, 2021, **11**, 1071.
10. W. J. Lee, Y. J. Hwang, J. Kim, H. Jeong and C. W. Yoon, *ChemPhysChem*, 2019, **20**, 1382.